JOURNAL of
MATERIALS and MECHATRONICS:A

e-ISSN 2717-8811
JournalMM, 2022, 3(2), 179-193
https://doi.org/10.55546/jmm.1129943

Araştırma Makalesi / Research Article

Characteristics and Corrosion Behavior of Sinter-Aluminized P/M Steels

Selvin TURGUT[1]*

[1] Republic of Turkey Ministry of Trade, General Directorate of Domestic Trade, Ankara, Turkey,
ORCID ID: https://orcid.org/0000-0001-6227-6182, selvinustabas@gmail.com

Geliş/ Received: 13.06.2022; **Kabul / Accepted:** 26.07.2022

ABSTRACT: In this study, the effects of different cold pressing pressures and sintering mediums on microstructure, micro hardness, and corrosion behavior of steels produced by powder metallurgy (PM) method from Distaloy SA powders, were examined. The PM samples were first subjected to two different cold pressing pressures being 150 MPa and 200 MPa, then to the sintering process in two different sintering mediums as aluminum and argon, for 5 hours at 1000°C. The densities and surface roughness of sinter-aluminized and only sintered samples were measured, and it was determined that their densities were increasing by the increase of cold pressing pressure and that their roughness was decreasing by the increase of cold pressing pressure. The determination of microstructural characteristics of PM samples was performed by the use of X-ray diffraction (XRD), scanning electron microscopy (SEM), and energy dispersive spectroscopy (EDS) devices. Corrosion tests were electrochemically conducted in 3.5 wt.% NaCl solution. It was determined that sinter-aluminized samples showed higher corrosion resistance than samples sintered in argon medium depending on the Fe_xAl_y phases forming on the sinter-aluminized samples. Thus, the sinter-aluminizing process is promising for using PM materials in corrosive environments.

Keywords: Powder Metallurgy, X-Ray Diffraction, Sinter-Aluminized, Corrosion.

*Sorumlu yazar / Corresponding author: selvinustabas@gmail.com

Bu makaleye atıf yapmak için /To cite this article

Turgut, S. (2022). Characteristics and Corrosion Behavior of Sinter-Aluminized P/M Steels. Journal of Materials and Mechatronics: A (JournalMM), 3(2), 179-193.

Sinter-Alüminize T/M Çeliklerin Özellikleri ve Korozyon Davranışı

ÖZET: Bu çalışmada, Distaloy SA tozlarından toz metalurjisi (P/M) yöntemiyle üretilen çeliklerin farklı soğuk presleme basıncı ve sinterleme ortamının mikroyapı, mikrosertlik ve korozyon davranışlarına etkisi incelenmiştir. P/M numuneler; 150 MPa ve 200 MPa olmak üzere iki farklı soğuk presleme basıncıyla presleme işlemi sonrası; alüminyum ile argon olmak üzere iki farklı sinterleme ortamında 1000 °C'de 5 saat sinterleme işlemine tabi tutulmuştur. Sinter-alüminyumlanmış ve sadece sinterlenmiş örneklerin yoğunluk ve yüzey pürüzlülükleri ölçülmüş olup yoğunluklarının soğuk presleme basıncının artmasıyla arttığı yüzey pürüzlülüğünün ise azaldığı belirlenmiştir. P/M numunelerin mikroyapısal özelliklerinin belirleme işlemi X- ışını kırınımı difraksiyonu (XRD), taramalı elektron mikroskobu (SEM) ve enerji dağılımlı X-ışını spektroskopisi (EDS) cihazları kullanılarak gerçekleştirilmiştir. Korozyon deneyleri elektrokimyasal olarak %3,5 NaCl çözeltisinde gerçekleştirilmiştir. Sinter-alüminyumlanmış numunelerin yüzeyinde oluşan FexAly fazlarına bağlı olarak argon ortamında sinterlenmiş numunelere göre daha yüksek korozyon direnci gösterdiği tespit edilmiştir. Dolayısıyla sinter-alüminyumlama işlemi P/M malzemelerin korozitif ortamlardaki kullanımları için umut vadetmektedir.

Anahtar Kelimeler: Toz Metalurjisi, X-Işını Difraksiyonu, Sinter-Alüminyumlama, Korozyon.

1. INTRODUCTION

Powder metallurgy (PM), used in producing advanced technology materials, is a technique used for powdering metals and metallic alloys through mechanical and physicochemical methods and producing work pieces utilizing pressure and temperature without melting the powders. It consists of mixing and pressing the powders obtained from metals and metallic alloys and then sintering them to form a bond among the powder particles (German, 1998; Xiao-Su and Shanyi, 2017; Wu et al., 2019). While the pressing process is generally performed at room temperature, the sintering process is performed under the melting temperature of the powder with the highest melting temperature among the powders in the mixture (generally 70°C) and in a protective atmosphere (German, 1998). The pressing process determines the mechanical and physical characteristics of the material, and the density of the piece differs as per the applied pressing pressure and mode of action (Xiao-Su and Shanyi, 2017).

The most critical factors in replacing conventional metal forming methods with powder metallurgy are low energy cost, low material production costs, and availing of the material at the maximum level. In addition, the method’s characteristics such as diversity, production of pieces in complex forms, microstructural and microchemical homogeneity increase its importance in the production of advanced materials (Çavdar and Çavdar, 2015). Nuclear power fuel elements, biomedical prostheses, aircraft brake linings, high-temperature filters, gears, Tungsten filament lamps, electric contacts, orthopedic equipment, rocket fuels, explosives, jet engine pieces may be provided as examples of pieces produced from metal powders by the PM method (Yazıcı and Çavdar, 2017; Alshammari et al., 2019; Sharma et al., 2019; Chávez et al., 2020).

The applications on the material surface are actualized to improve the material's functional characteristics such as physical, chemical, electrical, electronic, magnetic, or mechanical characteristics. In this context, new materials are produced by improving the metallic and non-metallic plating methods. In the industry, surface engineering methods based on plating processes such as painting, dipping, sol-gel processes, cold and thermal spraying, chemical and electrochemical methods (anodization, electroplating, electroless plating, and electrophoretic deposition), plasma-

assisted technologies, physical vapor deposition (PVD), chemical vapor deposition (CVD) are used in order to improve the surface characteristics of steels and alloys. The low setup cost in thermochemical processes, and the obtainment of equivalent surface characteristics enabled the use of this method in powder metallurgy (Erdogan et al., 2020; Turgut and Günen, 2020).

The thermochemical process is the process of diffusion on the surface of the metal and/or non-metal (B, N, Cr, Ti, V, Al etc.) atoms by the use of the thermal diffusion method at high temperatures in order to change the chemical and microstructure of the material's surface (Çavdar and Çavdar, 2015; Günen et al., 2015). Aluminum and its alloys stand out due to their easy accessibility, low density, chemical and physical compatibility, higher wear resistance as well as their superior corrosion resistance in many environments (Erdogan et al., 2020). As a result, depending on the process selected, the borides or intermetalides (aluminates, chromites) diffuse on the surface of the material by temperature activation and cause the change of material's surface and the formation of new phases (Choy, 2003; Mittemeijer and Somers, 2014; Çavdar and Çavdar, 2015; Günen et al., 2015; Erdogan et al., 2020). This change actualizes employing diffusion, unlike the processes such as electrolytic or vapor precipitation, and the layer covers the atoms of original material and foreign elements diffused on it. The construct, thickness, and composition of the new phases formed change depending on parameters such as composition and chemistry of initial materials, characteristics of substrate materials, temperature, exposure time, and gas pressure (Medvedovski, 2016). Depending on the atom diameter of the diffused element, two different surface modifications form. If the atom diameter of the diffused element is small, the substrate material diffuses, and interstitial solid solution or exterior layer forms, and if the atom diameter of the diffused element is large, a compound forms on the surface as in the chromizing and aluminizing. Thermochemical processes are used in many fields of application, such as machinery, automotive, toolmaking, petroleum drilling, mining, and defense (Çavdar and Çavdar, 2015).

Thermochemical processes or plating with diffusion are divided into impregnation with non-metals (carburizing, nitriding, nitrocarburizing, and boronizing) and impregnation with metals (aluminizing, chromizing, siliconizing, vanadiumizing, and berylliumizing) depending on the element diffused. The practice of aluminizing, one of the processes of impregnation with metals from among thermochemical processes, is a preferred method due to its characteristics such as simplicity, reliability, and economy. It was informed by many studies that the corrosion resistance of steels increases as a result of the aluminizing process (Xiang and Datta, 2006; Lu et al., 2019). The materials obtained from the aluminizing process have been interesting for industrial applications thanks to their many properties. Heating element in furnaces or dryers, power units and incinerator pipes, piston valve, exhaust manifolds, petrochemical facilities are some of the areas where these materials are used. The aluminizing process is divided into low activity and high activity aluminizing, depending on the temperature and activity of aluminizing. The low activity aluminizing process is actualized at high temperatures such as 950-1050°C for preserving operation time, and the high activity aluminizing process is actualized at low temperatures such as 700-900°C (Dubiel et al., 2008; Mojaddami et al., 2012).

This plating compound bonds to crystal structures and sublayers by strong and short covalent bonds with high thermodynamic characteristics. High lattice energy ensures more stability in crystal structures and a high covalent bond in solids. It correlates with the materials' chemical stability and integrity in mediums that may damage the material. These platings, along with not covering free Fe and other elements, are not in free from in the elements added. Moreover, this prevents the possibility

of interaction of metals with the anions of the corrosive medium and ensures the increase of corrosion resistance (Grabke and Schutze, 1998; Ladd and Ladd, 1999).

When the studies in the literature were examined, Triani et al., in order to produce iron aluminite platings on stainless-steel substrates, obtained FeAl layers on the surface by performing the aluminizing process through exposing the stainless-steel substrates to thermochemical process in a slurry consisting of polyvinyl butyral, ethyl alcohol, Al, $AlCl_3$, and Al_2O_3 for 2, 4, 6 and 8 hours at 500-650°C. By the result of the study, it was specified that the homogenous FeAl layer of excellent ductility had formed by the increase of temperature and processing time and that this layer had significantly improved the oxidation resistance of the alloy (Triani et al., 2020).

Furthermore, in the study performed by Liu et al. in 2008, they explained the basic technological process of the hot-dip aluminized technique by emphasizing the features such as corrosion resistance, high temperature oxidation resistance. In addition, they summarized the applications of hot-dip aluminized steel in the field of engineering and gave information about its developing aspects (Liu et al., 2008).

Wang et al. (2018) used the single-stage powder pack method to prepare AIN/aluminized plating, having high corrosion resistance, on carbon steel. They examined the phase compositions by X-ray diffraction (XRD), and they examined the cross-sections by scanning electron microscopy (SEM) equipped with energy dispersive spectroscopy (EDS). They measured the corrosion resistance of AIN/aluminized plated sample by electrochemical test and expressed that the plating had improved the material's corrosion resistance (Wang et al., 2019).

Considering the studies performed in recent years, it has resorted to aluminizing process to improve the oxidation and corrosion resistance of the materials. High oxidation and corrosion resistance, provided for the material by the aluminum element, arises from the Al_2O_3 layer that continues to protect the primary metal as remaining on the material's surface. For this reason, superior oxidation and corrosion resistance through the Al_2O_3 layer, obtained through plating materials with aluminum in the medium of high temperature and different corrosive characteristics that the materials cannot resist, has become a more and more meaningful practice. For this purpose, in this study, the microstructure characteristics, hardness, and corrosion resistance -in different mediums- of samples of Distaloy powders that were produced with the PM method under two different pressures and that were sintered in different sintering mediums (Ar and Al), were examined and compared with each other. Considering the usage areas, the hardness and wear resistance properties of the material can be determined in further studies. In this way, the effect of the aluminizing process on hardness and wear is determined and studies for use are carried out.

2. MATERIALS AND METHODS

Initially, commercially available Distaloy SA powders with chemical composition Fe-1.84Ni-1.49Cu-0.8Zn-0.5Mo-0.5C-0.6Zn, and 50-100 μm average grain size were subjected to mechanical alloying for 24 hours to obtain a homogeneous powder mixture. Then, the powder mixture was weighed and cold-pressed by applying different pressures (150 and 200 MPa) to produce samples with a diameter of 40 mm, and thickness of 5 mm. The surfaces of the cold pressed samples were sanded with 320-1200 grit SiC paper before sintering, washed with distilled water and sonicated in methanol to obtain clean and smooth surfaces. The samples to be sintered in an argon environment were placed in crucibles made of stainless steel, their mouths were tightly closed and sintered at 1000°C for 5 hours. In the sintering process in aluminum environment, after the samples were placed

in a stainless-steel crucible, all sides were covered with a powder mixture of 45 wt.% Al + 45 wt.% Al_2O_3 + 10 wt.% NH_4Cl. Then, the mouth of the crucible was tightly closed and sintered for 5 hours by placing it in an electric muffle furnace preheated to the aluminizing temperature (1000 °C). After sintering in argon and aluminum environments, the crucible was removed from the furnace and the samples were left to cool at room temperature. Finally, the aluminized samples were removed from the crucibles and their surfaces were cleaned with a brush to remove any adhesion from the aluminum powder.

Process parameters and exemplary nomenclature for the samples are given in Table 1.

Table 1. Sample nomenclature and process parameters used in the process

Sample	Sintering Temperature (°C)	Sintering Medium	Pressing Pressure (MPa)	Sintering Duration (h)
S1	1000°C	Ar	150	5
S2			200	5
S3		Al	150	5
S4			200	5

The density measurements of the PM materials were determined by including the weights, measured in air and pure water, in the Equation 1. based on Archimedes' principle.

$$\rho = \frac{w_o \rho_w}{w_o - w'_o}$$

The surface roughness (Ra) of the samples was measured using a Wave System Hommelwerke T8000 2D profilometer. Surface roughness was determined as the average of 5 measurements made on each sample surface based on 1mm/s speed and 4mm length.

Metallographic samples were prepared with a precision cutting device for SEM, EDS, and XRD analyses by the end of the sintering and sinter-aluminizing process. Then, the samples were subjected to conventional grinding with 280-2500 SiC paper polished with 6 μm Al_2O_3 and 0.25 μm Al_2O_3 solution and then etched with 3 wt.% Nital solution to reveal microstructural details.

Metallographic studies were carried out on polished and etched cross-sections of the samples using Thermo Scientific Apreo-S SEM equipped with UltraDry EDS Detector and Quasor II EBSD system equipped with EDS. The thicknesses of the aluminite layers were measured by SEM, and the presence of phases (FeAl) formed on the surface of PM samples was identified by X-ray diffraction (XRD) analyses using a computer-controlled Rigaku SmartLab X-ray diffractometer. The diffraction patterns were obtained with Cu Kα radiation at a wavelength of λ = 0.154 nm over a 2θ range from 30° to 90°. Diffraction data were collected with 2.0 deg/min speed and step width of 0.02 degrees.

Corrosion characteristics of the samples were evaluated with the CHI 608E electrochemical workstation, controlled by a computer. A standard setup consisting of three electrodes, one platinum counter electrode, one Ag/AgCl electrode as a reference electrode, and one working electrode (1cm^2 exposed area) was selected for the corrosion assessment studies. All the corrosion tests were carried out using 3.5 wt.% NaCl aqueous solution. Open circuit potential (OCP) measurements of the samples were made over 3600s and plotted as a function of time after stabilization. Potentiodynamic corrosion tests were performed in the potential range of -250mV to +250mV at a scan rate of 0.1 mV/s. The Tafel extrapolation method was applied to reckon the corrosion current densities of the samples over

the linear portion of the anodic and cathodic graphs. The corrosion tests were repeated three times to ensure reproducibility, and the results were averaged.

3. RESULTS AND DISCUSSION

3.1 Density and Surface Roughness

The density and surface roughness values of Distaloy SA powder samples, which were initially pressed under two different pressures and were sintered in two different sintering mediums (Ar and Al), are given in Table 2.

Table 2. The density and roughness of the P/M specimens subjected to sintering and sinter-alumizing heat treatment

Sample	Density (gr/cm^3)	Relative density (%)	Surface roughness (Ra, µm)	Rz (µm)
S1	5.95	76.28	2.60	10.72
S2	6.02	77.17	2.27	9.54
S3	6.13	78.59	1.93	7.86
S4	6.18	79.23	1.75	7.66

When the density and surface roughness values of samples sintered in argon and aluminum mediums were examined as per the pressing pressures applied prior to sintering, it was determined that while the density values increased from 5.95 to 6.02, and from 6.13 to 6.18 by the increase of pressing pressure, the surface roughness values decreased from 2.60 to 2.27, and from 1.93 to 1.75, respectively. The density and surface roughness values of the samples differed as per the sintering medium. It was observed that density values were a bit higher and that the roughness values were lower along with filling of pores with aluminum in sinter-aluminized samples compared to samples sintered in Ar medium (Bagliuk, 2012; Sundaram et al., 2018).

The increase in the density of samples and the increase in pressing pressure may be explained by reducing air gaps among the powder particles. Gökmeşe et al., by their study performed in 2013, expressed that the density values were increasing along with the increase of pressure and that the pores among the particles were closing as the result of the pressing pressure applied from 250 MPa to 625 MPa on alloys prepared by the use powder metallurgy (Gökmeşe and Bostan, 2013).

Moreover, the surface roughness values of sinter-aluminized samples being lower compared to that of samples sintered in Ar medium may be attributed to the filing of porosity and gaps, remaining on the surface following cold pressing, with a secondary powder (sinter-aluminizing powder), and to the plating layer formed on the surface following the thermochemical process.

Considering these factors that affect the density and surface roughness, as the S4 sample is a sample that was sinter-aluminized and pressed under high pressing pressure, it has the highest density and lowest surface roughness among all the samples.

3.2. Characterization of Microstructure

SEM microstructure images, and EDS analyses of Distaloy steel PM samples, sintered for 5 hours in Ar medium are given.

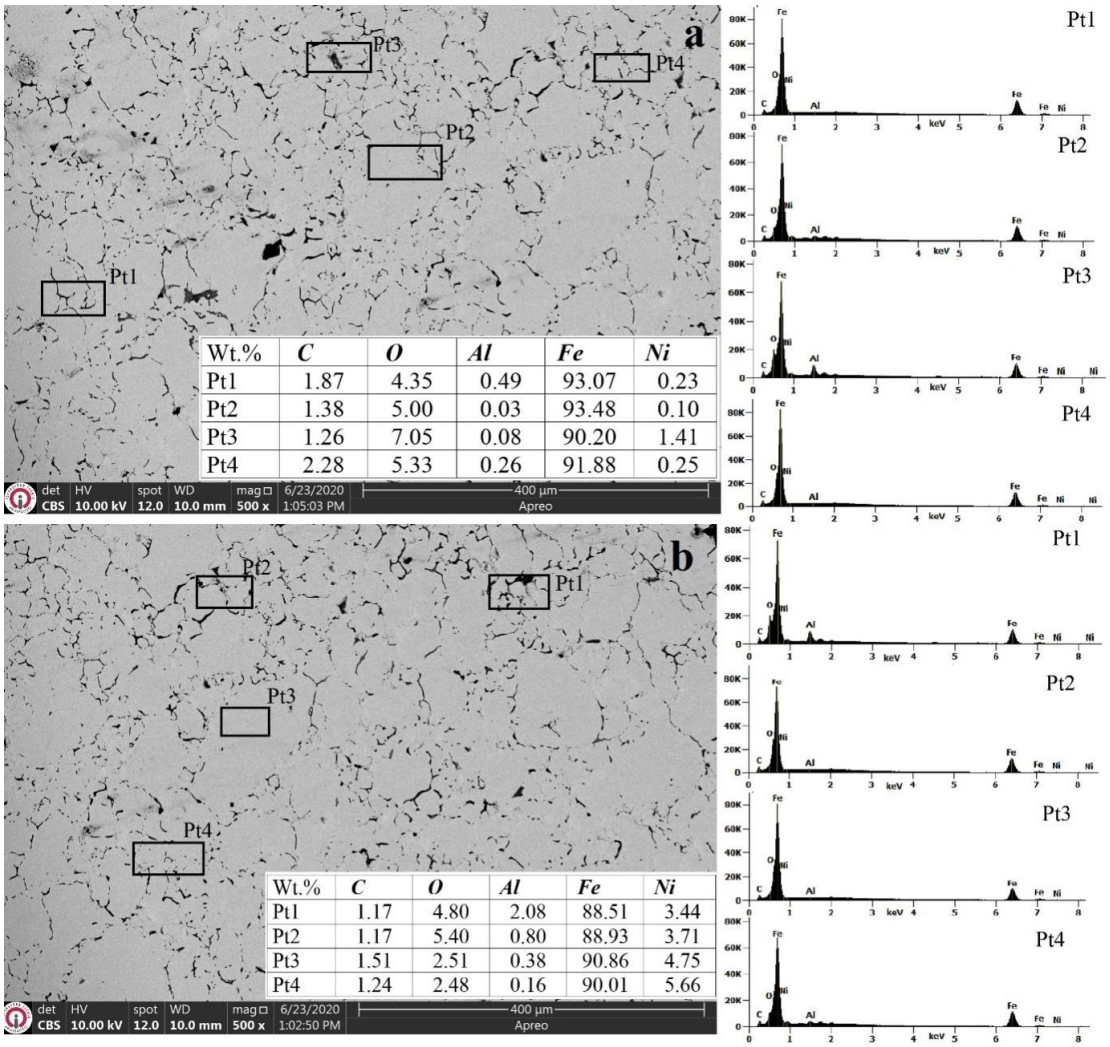

Figure 1. SEM microstructure view and EDS analysis of produced from Distalloy powders by P/M method a)150 MPa, b) 200 MPa pressing pressure after 5 hours at 1000 °C in Ar environment

As seen in Fig. 1, it was observed that the sample generally exhibited a homogenous distribution, but at some parts of the microstructure, oxide areas were being the characteristic of iron-based materials produced by powder metallurgy. Despite a decrease in the oxide contents (Fig. 1b EDS point) by the increase of pressing pressure from 150 MPa to 200 MPa, they were not completely removed. Due to the reduction of air gaps among powders and the increasing pressing pressure, the porosity decreased, and the density increased. Furthermore, the chemical bond formation among powder metal pieces is more substantial (Gökmeşe and Bostan, 2013; Turgut and Günen, 2020).

Moreover, by examining EDS analyses of the samples, it was observed that the construct was substantially comprised of iron and that low rates of carbon, oxygen, aluminum, and nickel were also present in the construct. It was also determined that the oxide content of the samples was 2.48-7.05 wt.%.

In Fig. 2, SEM images and EDS analyses of samples of Distaloy powders, subjected to cold pressing under 150 MPa and 200 MPa, and sinter-aluminizing for 5 hours at 1000°C, are given.

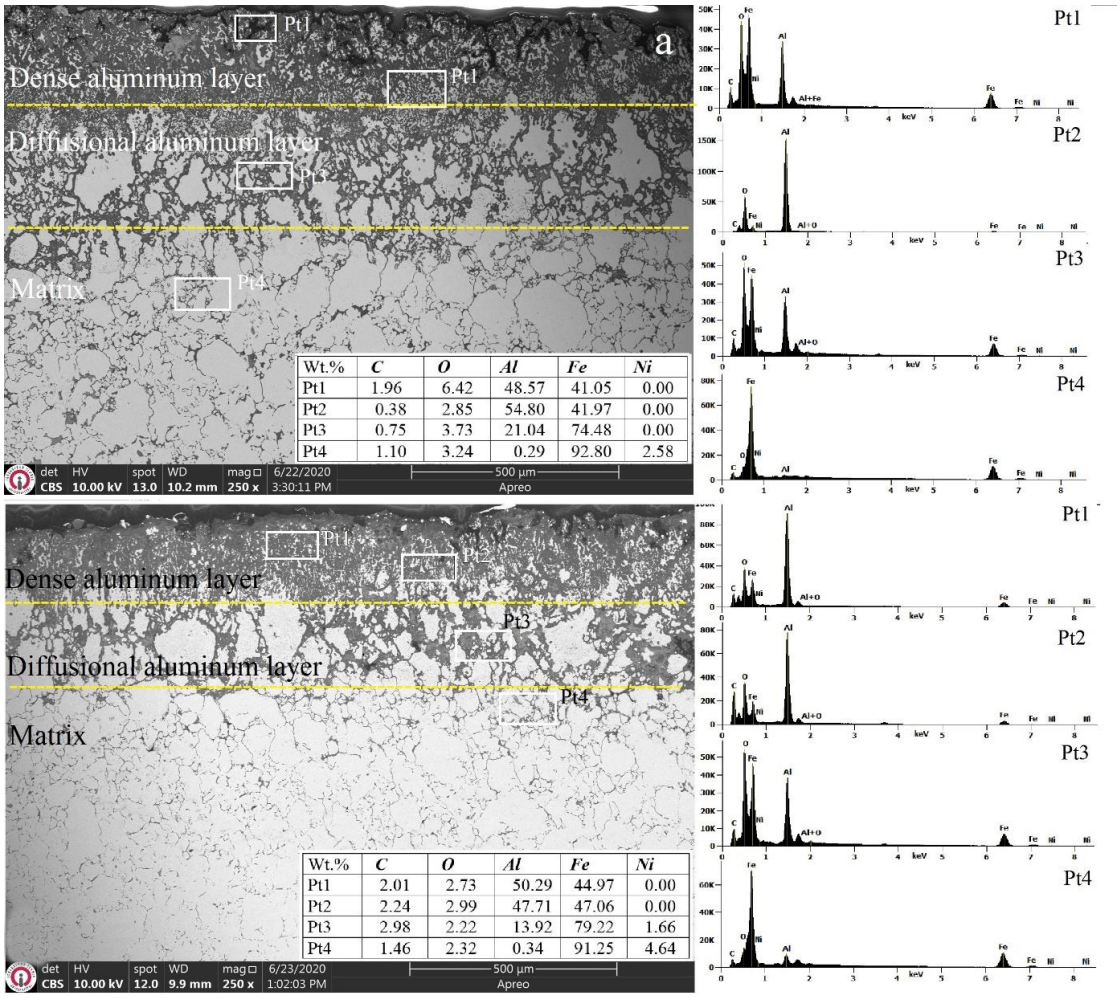

Figure 2. SEM microstructure view and EDS analysis of produced from Distalloy powders by P/M method a) 150 MPa b) 200 MPa pressing pressure after 5 hours at 1000 °C in a sinter-aluminizing medium

When the sectional views of samples, subjected to a sinter-aluminizing process for 5 hours period in Al medium by the use of 10 kV energy in scanning electron microscopy (SEM), were examined, it was observed that 3 different areas formed on the surface of the samples. These areas were i) intense aluminizing area, ii) diffusional aluminizing area, and iii) matrix area not affected by the aluminizing process. Moreover, EDS analyses were obtained from different points of plating layers and the matrix of each sample. It was determined that the contents of layers located at the plating area, being precise in the results of the metallographic examination, were exhibiting differences (Kayali, 2013).

The FeAl layer obtained was examined in terms of content, while about 47.71-54.80 wt.% Al was determined at the dense area, the Al rate at the diffusional area was determined as 13-21 wt.%. It was observed that the concentration of Al element decreased from the plating layer's outmost surface towards the matrix and that the plating layer concentrated in places. These areas, where the Al element concentrated, were the gray areas also observed in the results of EDS analysis, and this status conforms with the FeAl platings obtained in literature (Maki, 2019; Perez et al., 2002).

By the end of the plating process, it was determined that the thickness and contained phases of the plating layer formed on Distaloy SA steel did not differ. It was observed that the thickness of the diffusion layer, formed in samples subjected to the sinter-aluminizing process, was similar to that of samples subjected to different sintering periods. The cause of having no change in the diffusion layer

thickness is the uniformity of sintering temperature. Diffusion speed is directly proportional with temperature, and changes to be made in sintering temperature will change the concentration of diffused aluminum, and accordingly, it causes changes in the layer thickness (Callister, 1991; Li et al., 2008).

When the plating players obtained were examined in terms of morphology, it was determined that aluminum atoms were not intense on the surface as in the aluminizing layers obtained on the alloys produced through casting and forging. This status may be linked to accumulation at a place of aluminum atoms among powders bonded to each other only with mechanical bonds due to powder metallurgy process and their diffusion towards more inner parts instead of making chemical bonding with the elements there. Hence, the obtainment of iron-aluminum layers, which were much thicker than casting and forging alloys, supports this matter.

3.3. XRD Analyses

XRD analyses of samples produced with the PM method and sintered in Ar and Al mediums were performed, and the phase matching of the results obtained was actualized by using the library in PDXL software (Fig. 3).

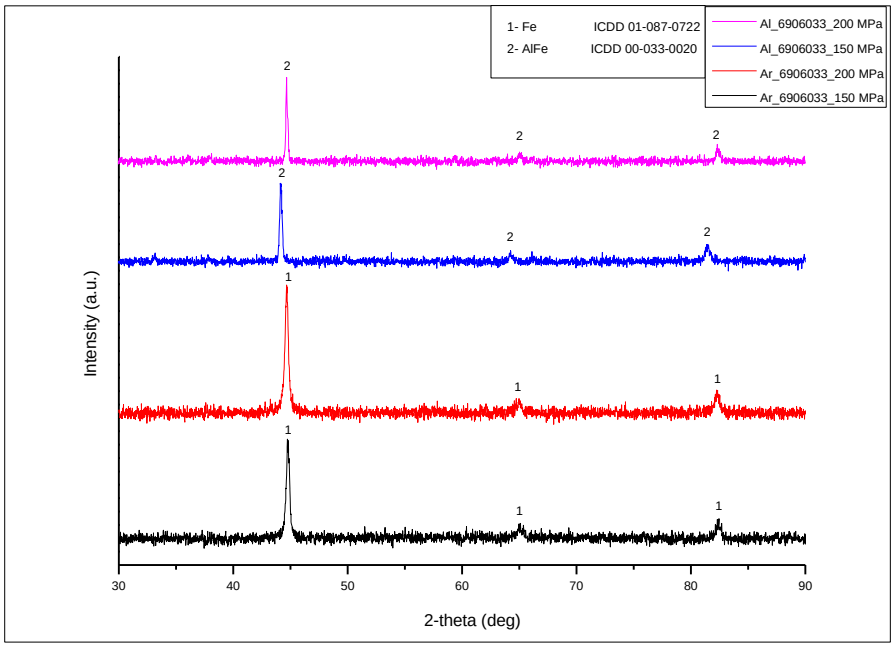

Figure 3. XRD diagram of samples produced from Distalloy SA powders and sintered in aluminum medium

As the result of examining X-ray diffraction (XRD) patterns, it was determined that the dominant phases on Distaloy SA steels produced under different pressing pressures and sintering mediums varied. As the result of XRD analyses, the primary Fe and FeAl compounds were determined. In samples subjected only to the sintering process, Fe phase, in the 229: Im-3m space group with card number ICDD: 01-087-0722, was dominant on the construct. This phase corresponded to peaks at angle values 44, 64, 82 in the XRD diagram.

Moreover, in the samples subjected to a sinter-aluminizing process for 5 hours at 1000°C, characteristic peaks of the construct, at angle values of 44, 64, and 81 of the FeAl phase with card number ICDD: 00-033-0020, were obtained. The phase desired to form in the aluminum plating process by the thermochemical method is the FeAl phase being present at the part rich in iron on the

Fe-Al balance diagram. In the study performed, the presence of this phase was observed. In the aluminizing process, it is avoided from the formation of phases with high Al content as they increase the fragility of the aluminite layer and decrease the oxidation resistance. FeAl phase, forming on the surface of the plating layer, has a high melting point, high resistance, high hardness, high corrosion and oxidation resistance, high elasticity module, and high electric resistance (Martinez et al., 2006).

3.4. Corrosion Analyses

The corrosion resistance of samples produced by sintering of Distaloy SA 6906033 powder in two different mediums (Ar and Al) was evaluated using open circuit potential measurement and potentiodynamic polarization curve measurement. The graphs of samples' corrosion tests, performed in 3.5 wt.% NaCl solution is given in Fig. 4.

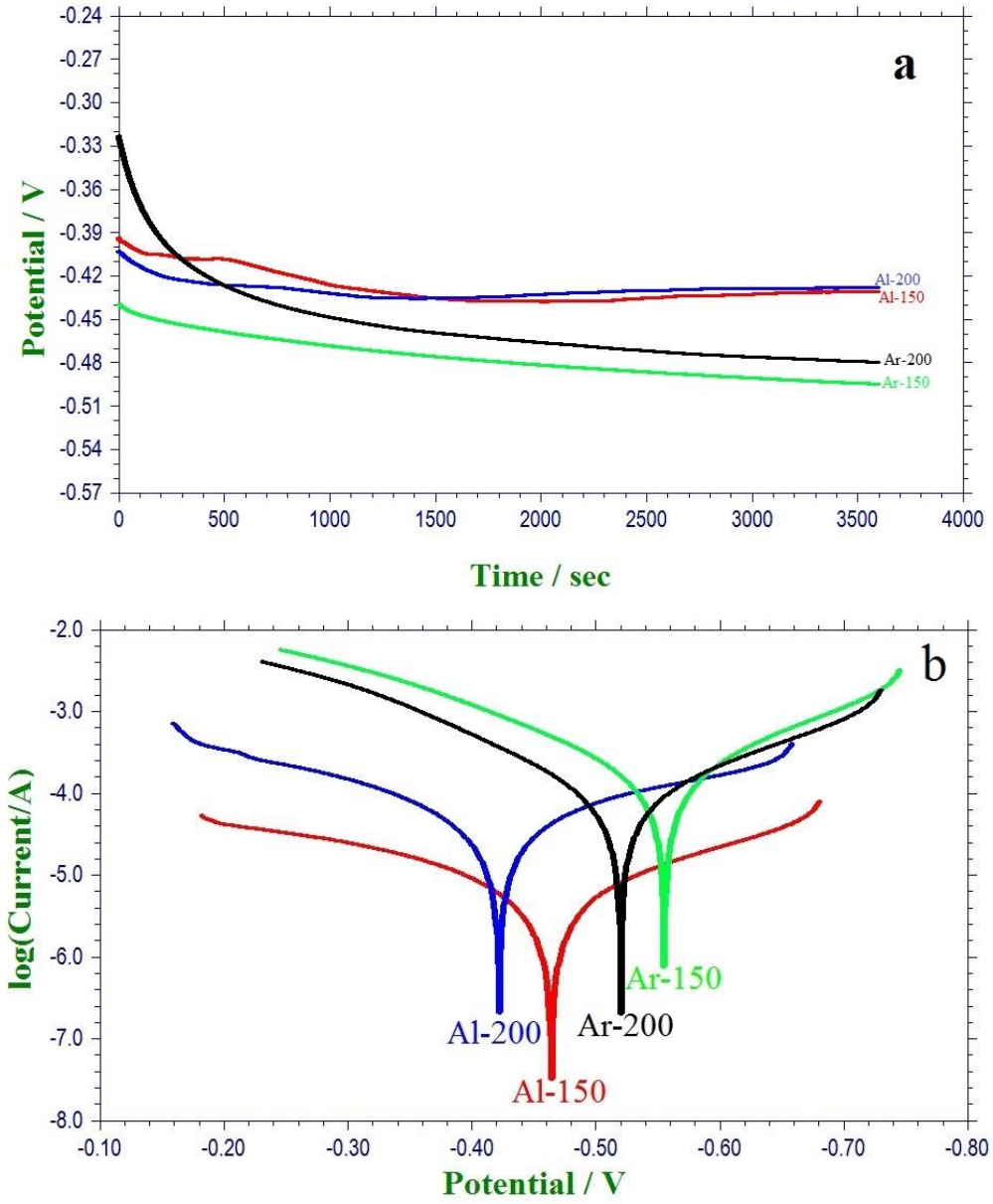

Figure 4. a) OCP curves, b) Tafel curves in NaCI solution of the sintered and sinter-aluminized samples

The potential value is measured in the OCP technique while no current passes from the circuit. The potential value, measured from an ionic solution, is the balance potential of the cathodic and

anodic reactions. Potential difference values, forming due to metal corrosion in a corrosive environment, are recorded as corrosion potential (Figure 4a). It is known that the corrosion resistance of samples of curves, being closer to the positive side on the OCP graphs, is higher (Öztekin, 2014).

When Figure 4a is examined, while samples subjected to sinter-aluminizing were at the narrow range from -0.39 to 0.42 V, it is observed that the samples subjected only to sintering continuously decreased as beginning from -0.33 V towards the potential of -0.48 V, and that they did not reach a stable course by the end of 3600 sec. This status revealed that the samples subjected to sinter-aluminizing were positioned on a more positive side than the samples subjected only to sintering and that they were more stable, and thus their corrosion potential was lower. The corrosion potential exhibited a decrease in Ar-200; Ar-150; Al-150; Al-200, respectively.

Considering the studies in literature, it was expressed that a passive aluminum film was forming on the surfaces of the steel samples through plating with aluminum and that it did not cause a significant change in the anode reaction while slowing down the cathode reaction. Moreover, as a result, they specified that a decrease occurred in the corrosion potential determined by the balance between the two reactions (Chen et al., 2007; Heakal et al., 2011).

The semi-logarithmic current-potential curves, drawn in anodic or cathodic direction as beginning from the corrosion potential, are known as Tafel curves. The current, where the point -on the corrosion potential-, where the Tafel curves intersect -when their linear parts are reversely extrapolated-, is determined, is the corrosion current (Öztekin, 2014). The extrapolation of Tafel curves, Ecorr (corrosion potentials), Icorr (corrosion current), and corrosion speed were calculated, given in Table 3. Ecorr value represents the samples' thermodynamic tendency for corrosion, and Icorr value represents the corrosion rate. The Ecorr values of Ar 150, Ar 200, Al 150, and Al 200 samples were -0.555 V, -0.520V, -0.464V, and -0.422V, respectively; and their Icorr values were $1.56x10^{-4}$ μAcm^{-2}, $8.52x10^{-5}$ μAcm^{-2}, $5.54x10^{-6}$ μAcm^{-2}, and $4.50x10^{-5}$ μAcm^{-2}, respectively. It was observed that the Ecorr values of samples subjected to sintering in argon medium were lower compared to the Ecorr values of samples subjected to sinter-aluminizing. Furthermore, this indicates that the corrosion resistance of PM samples subjected to sintering in Ar medium are lower than samples subjected to sinter-aluminizing.

Table 3. The E_{corr} (corrosion potential), I_{corr} (corrosion current density), and corrosion rate values were determined from the polarization curves

Sample	Solution	Ecorr (V)	Icorr (μAcm^{-2})	Corrosion rate (gr/h)
Ar 150	%3.5 NaCl	-0.555	$1.56x10^{-4}$	$16.30x10^{-5}$
Ar 200		-0.520	$8.52x10^{-5}$	$8.90x10^{-5}$
Al 150		-0.464	$5.54x10^{-6}$	$0.58x10^{-5}$
Al 200		-0.422	$4.50x10^{-5}$	$4.70x10^{-5}$

When Tafel graphs were examined, it was observed that the samples subjected to sinter-aluminizing were positioned more to the right compared to samples subjected only to sintering as in the OCP graphs. This status conforms with the Ecorr values given in Table 4. However, it was observed that the Al-200 sample, which was positioned at the rightmost side in terms of Ecorr values, did not exhibit the lowest corrosion current ($4.50x10^{-5}$) and that the Al-150 sample exhibited the lowest corrosion current as $5.54x10^{-6}$. This status indicates that the samples' log (current/A) values are essential and their Ecorr values in corrosion losses. Because the lowest log (current/A) values were determined in the Al-150 samples among all the samples, and it was the sample in which the

corrosion losses were the lowest. The Icorr values of samples subjected to sinter-aluminizing were lower than the samples subjected only to sintering, and their corrosion resistance was higher. Briefly, in terms of the corrosion resistance of samples produced from Distaloy SA 6906033 powder by the sinter-aluminizing process, an improvement was ensured at the range of 1.90 times (Ar-200/Al200) and 15.34 times (Ar-200/Al-150) compared to samples subjected only to sintering.

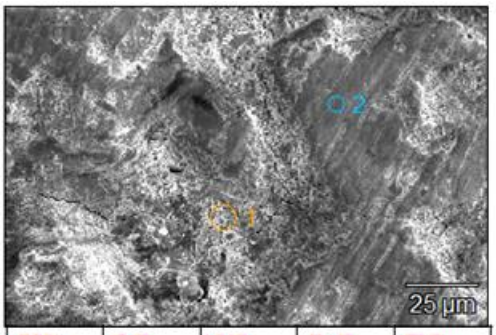

Wt %	C-K	O-K	Na-K	Si-K
Pt-1	2.14	30.82	0.00	0.22
Pt-2	1.67	34.21	0.00	0.07

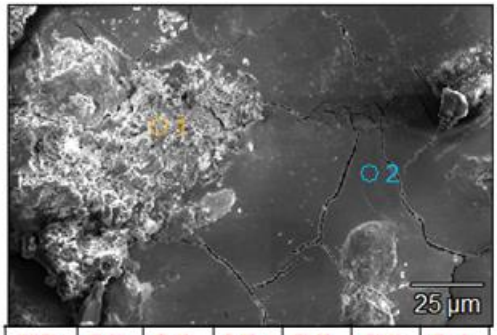

Wt %	C-K	O-K	S-K	Si-K	Cl-K	Fe-L
Pt-1	5.34	32.53	0.27	0.65	2.51	58.70
Pt-2	1.47	34.31		0.20	2.39	61.63

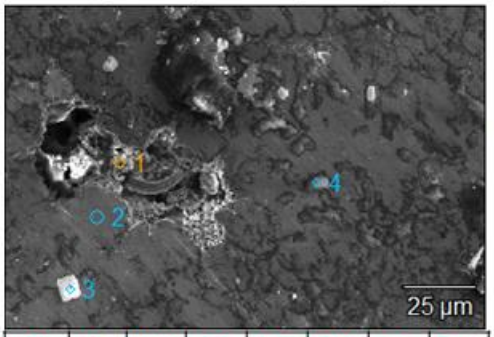

Wt %	C-K	O-K	Na-K	Al-K	Si-K	Cl-K	Fe-L
Pt-1	13.9	24.70	2.04	42.07	0.50	1.70	15.08
Pt-2	1.35	0.83	0.24	8.33	0.10	0.07	89.08
Pt-3	2.27	5.77	30.92	6.24	0.36	41.44	13.00
Pt-4	0.00	9.37	2.34	86.42	0.34	1.52	0.00

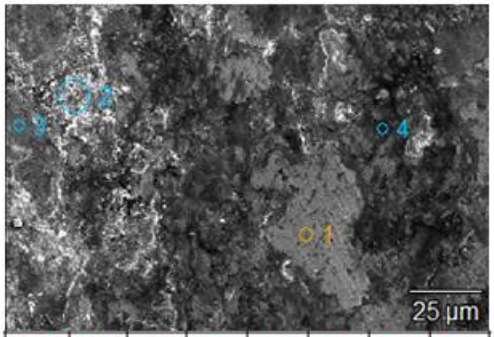

Wt %	C-K	O-K	Na-K	Al-K	Si-K	Cl-K	Fe-L
Pt-1	2.27	1.34	0.00	1.11	0.19	0.11	94.98
Pt-2	8.37	25.69	7.18	0.36	0.36	11.17	46.87
Pt-3	2.48	30.70	1.37	0.11	0.24	2.02	63.08
Pt-4	11.4	11.54	2.20	19.19	0.24	1.96	53.45

Figure 5. a) Ar medium, b) sintered in Al medium SEM and EDS views taken after corrosion treatment in NaCl solution of samples

When the SEM images of samples after corrosion were examined, it was observed that crevice corrosion had formed on the surface of samples subjected to sintering in argon medium and that pitting corrosion formed on the surface of samples subjected to the sinter-aluminizing process. For the development of pitting corrosion, the presence of halogen ions is required in the medium. In the study performed, NaCl was preferred as the corrosion medium, and Cl ions had caused pitting corrosion. This corrosion begins with an anodic reaction formed at any point of the metal surface, and by the effect of environmental conditions, the anodic reaction continues by a series of autocatalytic reactions that give rise to each other and causes the formation of the pit at that point.

The higher Ecorr values of samples subjected to sinter-aluminizing, compared to samples subjected only to sintering, indicate better corrosion resistance. Al-150 sample exhibited the lowest Icorr value ($5.54x10^{-6}$ μAcm^{-2}) attributed to the thick and relatively less porous plating surface. Al-200 sample had a higher Icorr value ($4.50x10^{-5}$ μAcm^{-2}) than the Al-150 sample, and the reason for this was the presence of relatively larger pores and micro-cracks on its surface.

4. CONCLUSION

Distaloy SA 6906033 alloys were pressed with cold pressing method under the pressures of 150 MPa and 200 MPa, and they were subjected to sinter-aluminizing process and only to sintering process for 5 hours at 1000°C. The changes in the microstructural, mechanical, and corrosion behaviors of samples obtained were examined.

While the densities of samples, sintered in argon and aluminum mediums, increased by pressing pressure, their surface roughness decreased. Considering the microstructure characteristics, while the Fe phase was dominant on the construct in samples subjected to sintering in argon medium, a surface structure forming of FeAl phase was subject in samples subjected to sinter-aluminizing. Porosity was present in both the samples subjected to sintering and sinter-aluminizing, and porosity decreased by the increase of cold pressing pressure, but it was not obliterated. Considering the corrosion behaviors, the corrosion potentials of samples subjected to sinter-aluminizing in NaCl medium were lower than those subjected only to sintering. Moreover, when evaluated among themselves, it was determined that the corrosion potential was decreasing along with the increase of cold pressing pressure (Ar-150 > Ar-200; Al-150 > Al-200). The lowness of Ecorr values, obtained as the result of corrosion tests, of samples subjected to sintering compared to samples subjected to only sinter-aluminizing, and the highness of Icorr values, obtained as the result of corrosion tests, of samples subjected to sintering compared to samples subjected to only sinter-aluminizing, indicate that these materials exhibit higher corrosion resistance. Sinter-aluminizing of Distaloy SA 6906033 alloys positively affected the material's corrosion resistance as well as its structural and mechanical characteristics. The actualization in a single step of the sintering process of the alloy along with aluminizing is essential in terms of processing time and energy. The study results indicated that the sinter-aluminizing process is promising in the usage of PM materials in corrosive environments.

5. CONFLICT OF INTEREST

Authors approve that to the best of their knowledge, there is not any conflict of interest or common interest with an institution/organization or a person that may affect the review process of the paper.

6. AUTHOR CONTRIBUTION

Selvin TURGUT has the full responsibility of the paper about determining the concept of the research, data collection, data analysis and interpretation of the results, preparation of the manuscript and critical analysis of the intellectual content with the final approval.

7. REFERENCES

Alshammari Y., Yang F., Bolzoni L., Low-cost powder metallurgy Ti-Cu alloys as a potential antibacterial material. Journal of the Mechanical Behavior of Biomedical Materials 95, 232-239, 2019.

Bagliuk G., Properties and structure of sintered boron containing carbon steels. Sintering–Methods and Products 12, 249-266, 2012.

Callister W. D., Materials science and engineering: an introduction (2nd edition). Materials & Design, 1991, https://doi.org/10.1016/0261-3069(91)90101-9.

Chávez J., Alemán O. J., Martínez M. F., Vergara-Hernández H. J., Olmos L., Garnica-González P., Bouvard D., Characterization of Ti_6Al_4V–Ti_6Al_4V/30Ta bilayer components processed by powder metallurgy for biomedical applications. Metals and Materials International 26(2), 205-220, 2020.

Chen X. H., Dong J. H., Han E. H., Ke W., Effect of Al alloying on corrosion performance of steel. Corrosion Engineering, Science and Technology 42(3), 224-231, 2007.

Choy K. L., Chemical vapor deposition of coatings. Progress in Materials Science 48, 57–170, 2003.

Çavdar P. S., Çavdar U., The evaluation of different environments in ultra-high frequency induction sintered powder metal compacts. Revista de Metalurgia 51(1), e036, 2015.

Dubiel B., Moskalewicz T., Swadzba L., Czyrska-Filemonowicz A., Analytical TEM and SEM characterization of aluminide coatings on nickel based superalloy CMSX-4. Surface Engineering 24(5), 327-333, 2008.

Erdogan A., Kursuncu B., Günen A., Kalkandelen M., Gok M. S., A new approach to sintering and boriding of steels "Boro-sintering": Formation, microstructure and wear behaviors. Surface and Coatings Technology 386, 125482, 2020.

German R. M., Powder metallurgy of iron and steel. New York: John! Wiley & Sons Inc, 1998.

Grabke H. J., Schutze M., Oxidation of Intermetallics. WILEY-VCH Verlag GmbH: Berlin, Germany, 1998.

Gökmeşe H., Bostan B., The Effects of Pressing and Sintering on Pore Morphology and Microstructural Properties in AA 2014 Alloy. Gazi University Journal of Science Part C: Design and Technology 1(1), 1-8, 2013.

Günen A., Kurt B., Somunkıran İ., Kanca E., Orhan N., The effect of process conditions in heat-assisted boronizing treatment on the tensile and bending strength characteristics of the AISI-304 austenitic stainless steel. Physics of Metals and Metallography 116(9), 896-907, 2015.

Heakal F. E. T., Tantawy N. S., Shehta O. S., Influence of chloride ion concentration on the corrosion behavior of Al-bearing TRIP steels. Materials Chemistry and Physics 130(1-2), 743-749, 2011.

Kayali, Y., Investigation of the diffusion kinetics of borided stainless steels. Physics of Metals and Metallography 114, 1061-1068, 2013.

Ladd M., Ladd M. F. C., Crystal Structures: Lattices and Solids in Stereoview. Horwood Series in Chemical Science; Elsevier: Chichester, UK, 1999.

Li G. J., Wang J., Li C., Peng Q., Gao J., Shen B. L., Microstructure and dry-sliding wear properties of DC plasma nitrided 17-4 PH stainless steel. Nuclear Instruments and Methods in Physics Research Section B: Beam Interactions with Materials and Atoms 266(9), 1964-1970, 2008.

Liu X. M., Yi D. W., Liu B., Ma Z. W., Wang G. W., Current status and application of hot-dip aluminizing technique. Materials Protection-Wuhan 41(4), 47, 2008.

Lu C. H., Feng C., Han L. H., Feng J., Zhu L. J., Jiang L., Feng Y. R., Corrosion Behavior Research of Aluminized N80 Tubing in Water Injection Well. Materials Science Forum 944, 1035-1039, 2019.

Maki J., Corrosion Behavior of Aluminized Steel Sheets in 50-Year Outdoor Exposure Test. ISIJ International 59(10), 1870-1877, 2019.

Martinez M., Virguer B., Maugis P., Lacaze J., Relation Between Composition Microstructure and Oxidation in Iron Aluminidies. Intermetallics 14(10-11), 1214-1220, 2006.

Medvedovski E., Formation of corrosion-resistant thermal diffusion boride coatings. Advanced Engineering Materials 18, 11–33, 2016.

Mittemeijer E. J., Somers M. A. J., Thermochemical Surface Engineering of Steels. 1st ed. Elsevier-Woodhead Publishing: Cambridge, UK, 2014.

Mojaddami M., Rastegari S., Arabi H., Rafiee H., Effect of heat treatment on coating microstructure applied by high activity diffusion process on IN738L. Surface Engineering 28(10),772-777, 2012.

Öztekin K., Çinko Kaplanmış Karbon Çeliğinin Na-okzalat ve Na-tartarat Ortamlarında Polianilin ve Poli o-anisidin ile Kaplanarak Korozyon Direncinin Geliştirilmesi, Mustafa Kemal Üniversitesi Fen Bilimleri Enstitüsü,Yüksek Lisans Tezi (Basılmış), 2014.

Pérez F. J., Pedraza F., Hierro M. P., Balmain J., Bonnet G., Comparison of the high-temperature oxidation of uncoated and CVD–FBR aluminized AISI-304 stainless steel. Oxidation of Metals 58(5), 563-588, 2002.

Sharma B. P., Rao G. S., Vates U. K., Powder Metallurgy Processing and Mechanical Characterization of Iron-Based Composite Reinforced. Advances in Industrial and Production Engineering: Select Proceedings of FLAME 2018 303, 2019.

Sundaram M. V., Surreddi K. B., Hryha E., Veiga A., Berg S., Castro F., Nyborg L., Enhanced densification of PM steels by liquid phase sintering with boron-containing master alloy. Metallurgical and Materials Transactions A 49(1), 255-263, 2018.

Triani R. M., Gomes L. F. D. A., Aureliano R. J. T., Neto A. L., Totten G. E., Casteletti L. C., Production of aluminide layers on AISI 304 stainless steel at low temperatures using the slurry process. Journal of Materials Engineering and Performance 29(6), 3568-3574, 2020.

Turgut S., Günen A., Mechanical Properties and Corrosion Resistance of Borosintered Distaloy Steels. Journal of Materials Engineering and Performance 29(11), 6997-7010, 2020.

Wang X. Y., Du J. J., Ma Z. W., A One-Step Pack Cementation Method for Preparing AlN/Aluminizing Coating with Good Corrosion Resistance. Solid State Phenomena, 295, 3-8, 2019.

Wu J., Ma B., Li H., Stanciulescu I., The running-in micro-mechanism and efficient work conditions of Cu-based friction material against 65Mn steel. Experimental Techniques 43(6), 667-676, 2019.

Xiang Z. D., Datta P. K., Relationship between pack chemistry and aluminide coating formation for low-temperature aluminisation of alloy steels. Acta Materialia 54(17), 4453-4463, 2006.

Xiao-Su Y., Shanyi D., Litong Zhang Editors, Composite Materials Engineering. Volume 1, Fundamentals of Composite Materials, 2017.

Yazici A., Çavdar U., A study of soil tillage tools from boronized sintered iron. Metal Science and Heat Treatment 58(11-12), 753-757, 2017.